Atomic structure of the Cu/Si(111) interface by high-energy core-level Auger electron diffraction

S. A. Chambers
Department of Chemistry, Bethel College, St. Paul, Minnesota 55112

S. B. Anderson
Department of Physics, Bethel College, St. Paul, Minnesota 55112

J. H. Weaver
Department of Chemical Engineering and Materials Science, University of Minnesota, Minneapolis, Minnesota 55455
(Received 14 February 1985)

High-energy core-level Auger emission from adsorbed atoms on single-crystal surfaces is accompanied by diffraction and interference effects, similar to those observed in x-ray photoemission. We have used azimuthal anisotropies in the Cu(LMM) intensity at shallow polar angles and a kinematical scattering model to determine the atomic geometry of the annealed one-monolayer-thick Cu/Si(111) interface. The calculated azimuthal intensity distributions are a very sensitive function of surface geometry. Optimal agreement with experiment occurs when the ideal unreconstructed Si(111) surface is allowed to reconstruct to a planar geometry and Cu atoms are placed in hollow sites at a depth of 0.1±0.1 Å below the surface plane.

I. INTRODUCTION

A variety of photoelectron diffraction techniques have recently been shown to be useful tools for studying surface structures.[1-7] In general, different surface geometries are modeled and photoelectron scattering formalisms are used to calculate the angular intensity distributions to compare with experimental results. One approach is to use conventional x-ray sources so that high-energy photoelectron scattering from near-neighbor atoms will be focused largely in the forward direction. It is then possible to use a kinematical scattering formalism for interpreting the observed anisotropies, thereby greatly simplifying the calculations.[2] A second approach is to use high-energy core-level Auger electrons. Indeed, a number of recent articles have shown that for comparable kinetic energies in excess of several hundred eV, the angular intensity distributions accompanying x-ray photoemission and core-level Auger emission are the same.[8-10] Together, these results show that the intensity modulation is indeed a final-state effect and is independent of the emission process. Moreover, the positions of zeroth-order forward-scattering features are essentially independent of electron kinetic energy, provided forward scattering predominates.[10]

Angle-resolved Auger and x-ray photoemission diffraction techniques have been used most often to study gas-metal systems with very good success.[1-7,9] However, very recently these techniques have been applied to metal-metal and metal-semiconductor systems as well.[11-13] In most cases, model systems with geometries previously assigned by other techniques have been the objects of investigation, thus establishing the validity of the technique.[1,2,5-7] In this paper, we apply the technique to a metal-semiconductor system which has not been extensively studied at the one-monolayer level and for which the surface structure is not known: Cu/Si(111). The only avail-

able surface structural information for the Cu/Si(111) system is an unusual LEED pattern which we and others have observed.[14] The pattern is essentially that of Si(111)1×1 with each integral beam surrounded by a smaller set of six spots, resembling what might be expected from a 5×5 overlayer periodicity. As we will show, by using Auger electron diffraction and associated kinematical calculations, we will deduce information about the local structural environment of the emitter.

II. EXPERIMENTAL DETAILS

Our spectrometer consists of a single-pass cylindrical mirror analyzer with angle-resolving capability which can be used for either angle-resolved Auger spectroscopy or LEED. For LEED measurements, we simultaneously ramp the electron gun accelerating voltage and analyzer mirror voltage so as to be always analyzing the elastic peak. The angle of incidence is set to 90°, resulting in a collection angle (θ) of 48° relative to the surface plane. The azimuthal angle (ϕ) is then varied to examine different portions of the reciprocal space of the surface. The resulting intensity versus primary energy spectra provide accurate mappings of diffracted beams. Angular variations are accomplished through the use of a precision two-axis goniometer which permits 360° rotations in the azimuthal angle ϕ and 100° variation in the polar angle θ. The precision in selecting either angle is ±1°.

The samples consisted of polished p-type (111)-oriented Si wafers. In vacuum, the wafers were repetitively Ar-ion sputtered and annealed to ~950° for 10 minutes, yielding an atomically clean, reconstructed 7×7 surface. This result was confirmed in a separate chamber equipped with conventional LEED optics. Polar and azimuthal angular calibrations were accomplished by using diffraction-induced Si(KLL) intensity maxima along low-index direc-

tions in the bulk material. The quality of the surface and the precision of the alignment are confirmed by the LEED *I-V* curves shown in Fig. 1. The symmetry of the surface is such that *I-V* curves in azimuthal planes containing the vectors designated by $\phi=0°$, 120°, and 240° should be identical, as should those in $\phi=60°$, 180°, and 300° and those in $\phi=30°$, 90°, 150°, 210°, 270°, and 330°. Also shown by arrows in Fig. 1 are the diffraction peak positions calculated using the Bragg equation for scattering from the first two layers of the ideal Si(111) surface. Diffracted beams corresponding to points in the reciprocal space of the surface layer are designated by Miller indices. Peaks resulting from diffraction from rows of atoms in the surface and subsurface layers are identified using the notations I' and I'' as described in the figure caption. As can be seen, the surface shows a high degree of structural regularity and the reproducibility of peak positions over the full 360° range confirms that the angular calibrations are accurate.

Evaporation of Cu was monitored with a quartz crystal oscillator. The pressure during evaporation rose from a base value of 4×10^{-11} Torr to $\leq2\times10^{-10}$ Torr. After deposition of 1 Å [1.1 monolayer (ML)] of Cu, the sample was annealed for a few minutes at 600 °C. Integrated Cu(MVV) peak intensities before and after annealing are within experimental error of one another. Thus, a one-to-one Cu to surface Si ratio still remains after annealing. After deposition and annealing, the crystal remained free of CO for at least three hours, depending on the temperature of the electron gun filament. During some of the azimuthal scans a partial monolayer of CO developed toward the end of the run. Replicate scans show that the only effect of the CO is an attenuation in signal; the diffraction modulation is unaffected except for a slight overall reduction in intensity.

All spectra were obtained using a primary beam voltage of 5 kV and an incident current of ≤0.5 μA. The resulting $N(E)$ spectra were smoothed and integrated after performing a linear background subtraction. In order to eliminate spurious intensity variations brought about by incident-beam current drift, each peak area has been divided by the number of counts in an arbitrary channel on the high-energy side of the peak. We have used this normalization technique to obtain Auger angular distributions from single crystals of known structure and have not found it to introduce any unwanted anisotropies. Azimuthal intensity scans were accomplished by collecting spectra every 4° and scans over a 128° range could be completed in three to four hours.

III. THEORETICAL CONSIDERATIONS

The problem of interpreting the observed anisotropies in terms of surface structure is accomplished through the
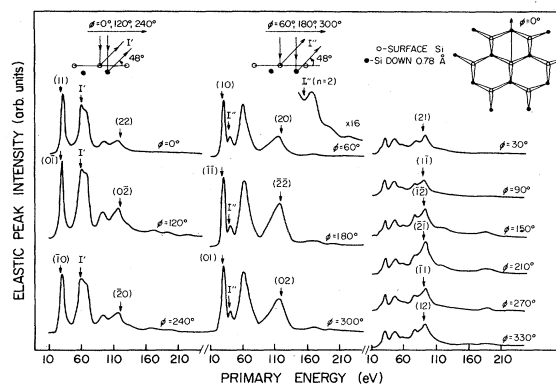

FIG. 1. Si(111)-7×7 LEED *I-V* curves in different azimuthal planes at a fixed collection angle of 48° relative to the surface. Diffracted beams originating in the surface layer are designated by Miller indices. Diffraction from atoms in the first and second layers gives rise to the beams I' and I'', as shown at the top of the figure.

use of a kinematical scattering formalism. A complete discussion of this formalism and its application to x-ray photoelectron diffraction has been published by Fadley.[15] Hence, only the essence of the theory and its application to the problem at hand are described in what follows.

As initially developed by McDonnell et al.,[16] the kinematical or single-scattering model of Auger emission assumes that the pre-scattering Auger electron can be treated as a spherical wave, provided the transition involves only core states. Upon reaching scattering centers, the spherical wave can be taken locally to be a plane wave, so long as the curvature of the electron wave over the dimensions of the scattering potential is small compared to the associated de Broglie wavelength. This condition is fulfilled at kinetic energies of several hundred eV. The scattering events themselves are described by a complex scattering factor $|f(\theta)|\exp[i\psi(\theta)]$ which can be calculated using the method of partial waves and free-atom or muffin-tin potentials. Thus, the Auger intensity for a given electron wave vector $\mathbf{k}$ is given by the superposition of the primary wave and waves scattered once from all other atoms in the vicinity of the emitter. Attenuation of the primary and scattered wave is included through the usual inelastic mean-free-path (λ) correction to the initial intensity. Finally, lattice vibrations are included via a Debye-Waller factor W, given by $\exp[-2k^2(1-\cos\theta)\times\langle u^2\rangle]$ where θ is the scattering angle and $\langle u^2\rangle$ is the mean-square displacement of the scatterer in its lattice site. The appropriate expression for the intensity of a given Auger electron with wave vector $\mathbf{k}$ is

$$I(\mathbf{k})\propto\left|\exp(-L/2\lambda)+\sum_i\frac{|f_i(\theta_1)|}{r_i}W_i\exp(-L_1/2\lambda)\exp\{i[kr_i(1-\cos\theta_i)+\psi_i(\theta_i)]\}\right|^2$$

$$+\sum_i\frac{|f_i(\theta_i)|^2}{r_i^2}(1-W_i^2)\exp(-L_i/\lambda)\,,$$

(1)

where the sum is performed over all atoms in a predefined cluster simulating the surface. L is the primary electron path length to the surface in the direction of $\mathbf{k}$ and r_i and θ_i are the emitter-to-scatterer distance and scattering angle of the ith scatterer, respectively. The second sum is needed to correct for the erroneous inclusion of Debye-Waller attenuation in "noncross" terms in the absolute square. That is, the product of a scattered wave with itself in the absolute square should not be attenuated by W_i^2 whereas products of waves scattered from different atoms should be.

The calculated intensities must be adjusted slightly for the effects of electron refraction at the surface. This correction amounts to a small change in polar angle given by

$$\theta' = \cos^{-1}\left[\left[\frac{E_k - V_0}{E_k}\right]^{1/2}\cos\theta\right], \qquad (2)$$

where θ' and θ are the propagation angles inside and outside the solid, E_k is the kinetic energy within the solid, and V_0 is the inner potential for the material. By comparison with experiment, the evaluation of Eq. (1) for all angles of interest and various choices of surface geometry is used to arrive at an optimal description of the surface structure.

For the problem at hand, we have used free-atom scattering factors calculated by Fink and Ingram[17] and Gregory and Fink.[18] Quadratic interpolation over energy from 500 to 1500 eV was done to arrive at suitable numbers for the Cu(LMM) Auger energy. Scattering factors for Si were obtained by linearly interpolating over atomic number between Al (Ref. 17) and P (Ref. 18) while those for Cu are found in Ref. 17. Previous work employing a kinematical model in the interpretation of angular-dependent XPS data[2] has shown that the calculated anisotropies are too large by about a factor of 2 and we have found the same to be true here. The probable reason for this discrepancy is the neglect of certain features in the theoretical treatment. These include (1) multiple scattering, which tends to increase the background between forward-scattering features, (2) anisotropic inelastic scattering, which requires a more sophisticated treatment of the inelastic mean free path, (3) spherical wave effects, which may be important for nearest-neighbor scattering at kinetic energies of ~ 1000 eV, and (4) surface defects, which are most surely present, yet are not included in the simulated cluster geometry. Therefore, we have reduced our free-atom scattering amplitudes by a factor of 2 prior to evaluation of Eq. (1) and have found agreement between theory and experiment to be much improved. In order to evaluate W_i we have used mean-square displacements obtained from Debye-temperature data for bulk Si and Cu.[19] A mean free path of 16 Å was used for the Cu(LMM) Auger electron (916 eV).[20] Finally, we have chosen an inner potential of 15 eV for the Cu/Si interface which is intermediate between that of pure Si (17 eV) and pure Cu (14 eV).

The substrate was simulated by various size clusters ranging from 100 Si atoms (10×10 on the surface) to 400 atoms ($10\times10\times4$). The calculated anisotropies were found to converge by a cluster size of $10\times10\times2$; the third and fourth layers did not contribute to the Cu(LMM) anisotropies. Simulation of the $8°\times8°$ spectrometer aperture was accomplished by constructing a 9×9 grid over the solid angle of acceptance and averaging intensities from the 81 points.

IV. RESULTS

In Fig. 2 we present azimuthal angular intensity distributions for Cu(LMM) emission at the polar angles 8°, 10°, 12°, 15°, 20°, and 48° relative to the surface plane. The ordinate scale on the right is based on integrated Auger peak areas. On the left, the intensities are measured in terms of anisotropy or percent deviation from the highest intensity (generally found at $\phi=0°$, 60°, or 120°). The error bars have a magnitude of two times the standard deviation of a set of four measurements taken at $\phi=124°$ for every azimuthal scan. Also shown in Fig. 2 is a representation of the surface to indicate how $\phi=0°$ is defined and a model of the surface as we think it exists.

Comparison of the azimuthal intensity distributions in Fig. 2 shows that anisotropies of 30% which exist at
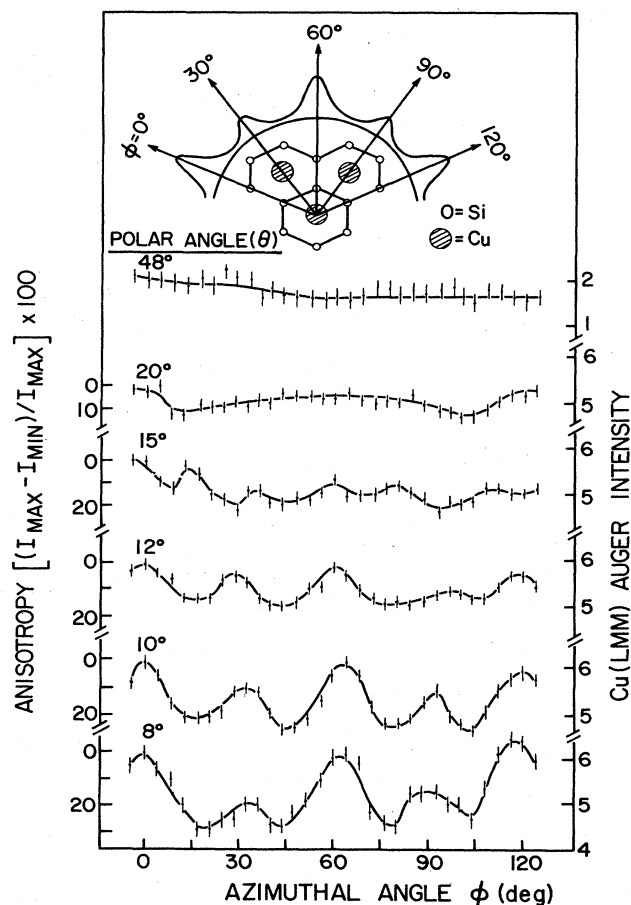

FIG. 2. Summary of Cu(LMM) azimuthal angular distributions at various polar angles for the annealed 1-ML Cu/Si(111) interface. At top, a picture of the surface is shown, indicating the azimuthal calibration. Intensity is expressed both in terms of integrated Auger intensities (right) and anisotropy (left).

$\theta = 8°$ drop off with increasing θ. By a collection angle of 48°, the profile is featureless. Moreover, the absolute Auger peak intensities decrease threefold from $\theta = 8°$ to $\theta = 48°$. The predominance of forward scattering allows us to draw qualitative conclusions about the structure of the surface. The large intensity maxima at $\phi = 0°$, 60°, and 180° at very low polar angles suggest that the Cu atoms reside in hollow sites and that forward scattering is occurring from nearest-neighbor Si atoms as indicated at the top of Fig. 2. The fact that the magnitude of the intensity is the same at 0° and 180° as it is at 60° suggests that the surface has reconstructed from the ideal "buckled" Si(111) structure to a planar structure with sixfold symmetry. The smaller peaks at 30° and 90° may result from zeroth-order diffraction from Cu atoms in neighboring hollow sites and first-order diffraction from nearest-neighbor Si atoms at $\phi = 0°$, 60°, and 120°.

Additional qualitative conclusions can be drawn from the fact that the anisotropy disappears at high polar angles, θ. This suggests that the Cu atoms are not deeply buried below the surface plane but rather are approximately in plane. Using the forward focusing behavior at the Cu(LMM) kinetic energy as a guide, deep burial of the Cu atoms would result in the coincidence of small Cu-to-surface-Si scattering angles and larger polar angles, generating large anisotropies at these angles. However, none are found. Further corroboration for this conclusion comes from the threefold increase in Cu(LMM) intensity as the polar angle is decreased from 48° to 8°. Polar intensity profiles of the 56-eV Cu(MVV) Auger transition from the annealed 1-ML Cu/Si(111) interface show that the peak intensity is essentially constant from $\theta = 90°$ to $\theta \simeq 10°$, at which point the intensity falls off rapidly.[21] At this low kinetic energy, multiple scattering dominates and forward focusing along near-neighbor internuclear vectors does not occur. Thus, the observed threefold increase in the 916-eV Cu(LMM) intensity from $\theta = 48°$ to $\theta = 8°$ can be attributed to extensive forward scattering and constructive interference in and near the surface plane. This can only result if the Cu atoms are situated approximately within the surface plane.

A quantitative structural assignment can be made by comparing the predictions of Eq. (1) for various choices of surface geometry with the observed angular profiles. In Figs. 3—5 we show the results of calculations assuming a rehybridized planar Si surface with Cu atoms in every hollow site at various z coordinates relative to the surface plane. Also shown are the experimental data overlapped with the theoretical curve for which the fit is best. For a polar angle of 8° (Fig. 3), the best fit occurs for a copper z coordinate (Z_{Cu}) of -0.05 Å. The peak positions and absolute intensities are in good agreement over the full range of azimuthal angles. The fit for the $Z_{Cu} = -0.10$ Å calculation is almost as good as that for $Z_{Cu} = -0.05$ Å, although the intensities of features at 0°, 60°, and 120° are too large relative to those at 30° and 90°. The fit to the calculation in which $Z_{Cu} = 0$ Å is reasonable, but those for 0.1 Å and -0.2 Å are very poor. On the basis of the data at $\theta = 8°$, it appears that $Z_{Cu} = -0.05 \pm 0.05$ Å.

Comparison of the $\theta = 10°$ data (Fig. 4) with the calcu-

lations also indicates that $Z_{Cu} = -0.05$ Å generates the best fit. Both peak positions and intensities agree very well. As in the 8° polar angle case, agreement for $Z_{Cu} = -0.10$ Å is also reasonable, though not as good as for -0.05 Å. For $Z_{Cu} < -0.10$ Å the features at 30° and 90° are too small relative to those at 0°, 60°, and 120°. For $Z_{Cu} = 0.0$ and 0.1 Å, the calculated intensity profiles are qualitatively different from experiment. Thus, it appears from the data at $\theta = 10°$ that $Z_{Cu} = -0.05$ to -0.10 Å.

The overall anisotropy in both theoretical and experimental curves is less at $\theta = 10°$ than at $\theta = 8°$ for $Z_{Cu} = -0.05$ Å, thus establishing the qualitative expectation of diminishing anisotropy at higher collection angles. This trend continues at $\theta = 12°$ (Fig. 5) with the experimental and theoretical anisotropies dropping further. At this collection angle, agreement between theory and experiment is best at $Z_{Cu} = 0.1$ Å, although one could argue that the fit for $Z_{Cu} = -0.20$ Å is not unreasonable. The situation is complicated by the lower intensity of the feature at $\sim 90°$ compared to that at 30°; the 0° to 60° section of the profile suggests -0.1 Å whereas the 60° to 120° section suggests -0.2 Å. $Z_{Cu} > -0.1$ Å leads to a poor fit, suggesting that -0.1 to -0.2 Å is the best choice based on the data at this polar angle.

For polar angles greater than 12°, the measured anisotropies decrease rapidly and become comparable to statistical uncertainties. Thus, we do not attempt to apply kinematical analysis to these angular distributions. Taken together, the results for 8°, 10°, and 12° suggest that under the influence of 1 ML of evaporated Cu annealed after deposition, the surface reconstructs to a planar arrange-
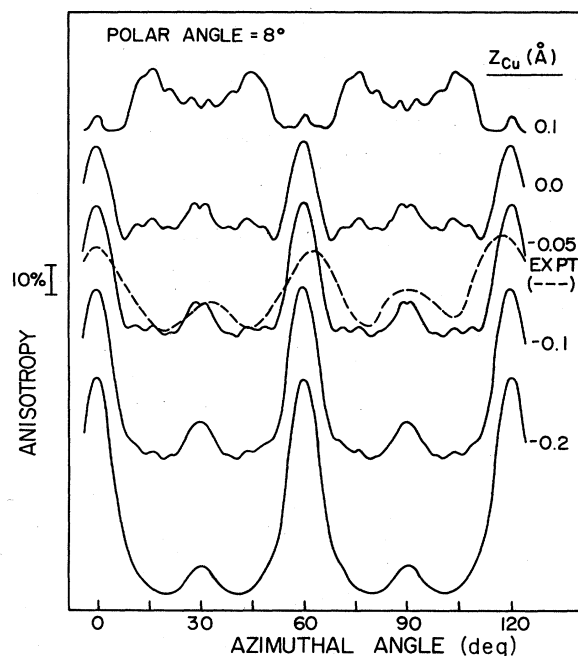

FIG. 3. Experimental and theoretical azimuthal intensity distributions for $\theta = 8°$. We have assumed a reconstructed planar surface Si surface with Cu atoms in every hollow site and have varied the Cu z coordinate. Experimental data has been overlapped with the theoretical curve it most closely resembles.

ment with sixfold symmetry and Cu atoms bind in every hollow site at a depth of -0.1 ± 0.1 Å.

V. DISCUSSION

A. Sensitivity of the method to structural details

Figures 3—5 illustrate that the calculated anisotropies are very sensitive to the choice of Z_{Cu} for the reconstructed geometry with Cu atoms in every hollow site. We now address the question of the sensitivity of the technique to the position of Si atoms and the concentration of Cu atoms on the surface. In Fig. 6 we show theoretical polar profiles for various choices of Si surface structure and number of Cu atoms per unit area. All calculations were done for $\theta=10°$ and the Cu atoms situated 0.05 Å below the surface plane. Also shown is the experimental azimuthal profile. The top curve assumes an ideal unreconstructed Si(111) structure and Cu atoms in every hollow site. In this geometry, Si atoms at $\phi=0°$ and 120° relative to the middle of the hollow site are depressed by 0.78 Å compared to those at 60° and 180° (see inset in Fig. 2). Thus, the Cu to Si scattering angle is much larger at $\phi=0°$ and 120° than at $\phi=60°$ and 180°. Forward scattering is then less pronounced, resulting in lower intensity. However, the experimental curve shows equal intensities at $\phi=0°$, 60°, and 120° as does the theoretical curve with the reconstructed surface. Moreover, additional features at ~15° and ~105° appear in the calculation which are the product of the constructive interference of several diffracted beams rather than simple forward scattering. These features are not present in the experimental data. Therefore the theory is indeed sensitive to the structure of the Si surface in which the Cu is embedded, and the ideal unreconstructed Si(111) structure does not fit well with
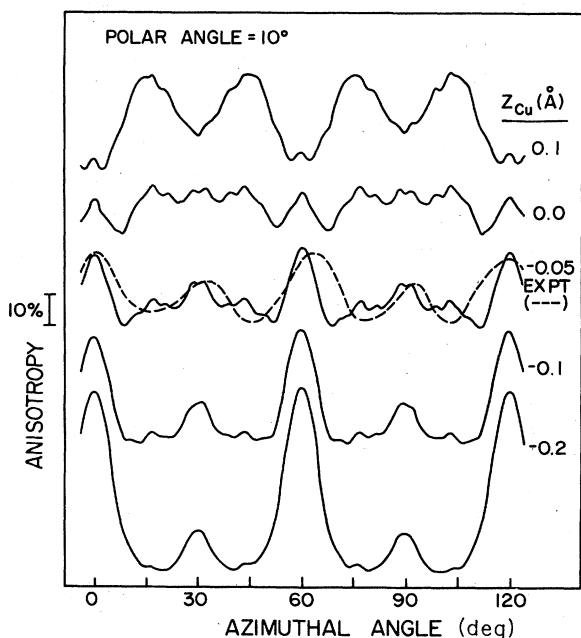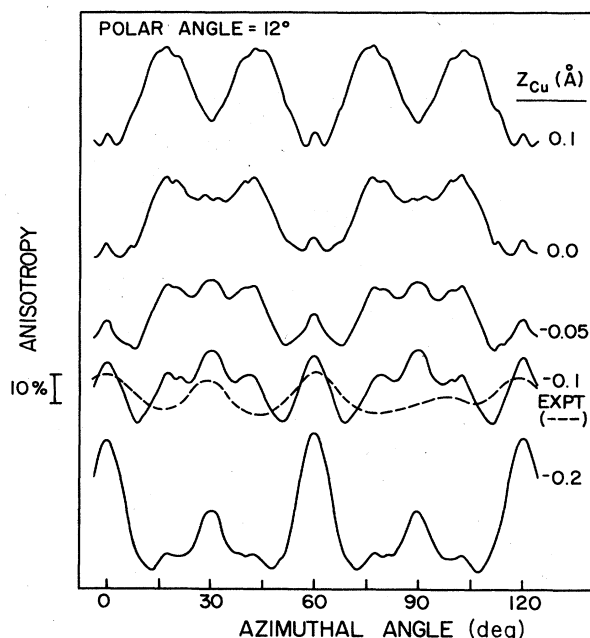

FIG. 5. Experimental and theoretical azimuthal intensity distributions for $\theta=12°$. Same geometry as in Fig. 3.

experiment.

The theory is also very sensitive to the number of Cu atoms per unit area on the surface. In the third theoretical curve from the top of Fig. 6 we have used the reconstructed geometry with Cu atoms in every other hollow site along $\phi=30°$ and $\phi=90°$, i.e., Cu scatterers are one hollow site removed from the emitter along $\phi=30°$ and 90°. The features at 0°, 60°, and 120° are modified in a minor way by the removal of every other Cu. However, the peaks at 30° and 90° grow considerably and agreement with the experiment becomes very poor. Further removal of Cu such that only the emitting Cu atom remains (bottom curve) does not significantly change the azimuthal

FIG. 4. Experimental and theoretical azimuthal intensity distributions for $\theta=10°$. Same geometry as in Fig. 3.
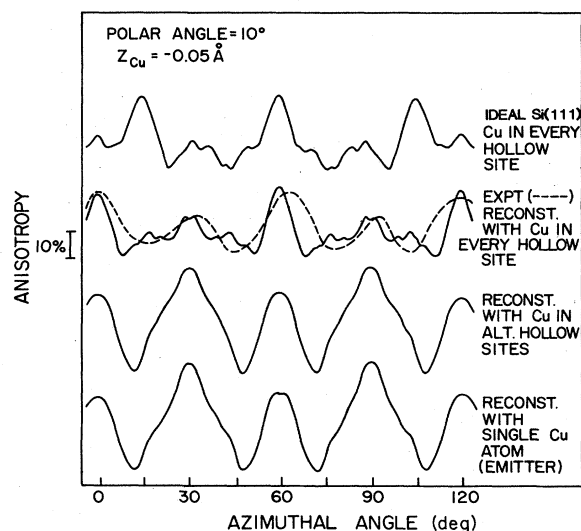

FIG. 6. Theoretical azimuthal intensity distributions for various choices of surface structure and Cu concentration on the surface.

pattern any further, thus establishing that the the observed scattering is indeed a local, short-range structural probe. This finding agrees well with similar calculations performed for a metal-metal interface.[12] In summary then, Fig. 6 demonstrates that optimal agreement between theory and experiment occurs only for the reconstructed Si surface Cu atoms in every hollow site.

B. Implications for surface electronic structure of Cu/Si(111)

The model we propose for the structure of the 1-ML Cu/Si(111) interface may involve a rehybridization of Si atoms in the surface bilayer from sp^3 to sp^2. This phenomenon would convert the dangling bond sp^3 orbitals to ordinary $3p$ orbitals normal to the surface. Such p orbital density could overlap with the $4s$ orbital of embedded Cu to form a subsurface resonance or sp surface state. Alternatively, surface bonding may be much less directional and instead involve the formation of bands.

Localized interaction between orbitals has been observed for the submonolayer Si(111)($\sqrt{3}\times\sqrt{3}$)R30°-Ag interface. Angle-resolved and angle-integrated UPS measurements show structure ~ 1 eV below E_F.[22,23] On the basis of DV-$X\alpha$ (discrete variational) cluster calculations with Ag embedded in the hollow sites, this feature can be attributed to back bonding between Ag $5s$, $5p$ orbitals and surface Si $3s$, $3p$ orbitals.[24] The direction of charge transfer is calculated to be from Si to Ag, in keeping with Pauling's electronegativities. Photoemission features at ~ 5.5 eV and 6.5 eV which are attributed to Ag $4d$ states are quite narrow, suggesting minimal interaction with surface Si atoms.[23] Partial-density-of-states calculations for a $Si_{13}H_{15}$ cluster with Ag embedded in the hollow sites indeed reveal that these states are largely Ag $4d$ in character with a very small admixture from nearest-neighbor Si atoms.[24] The geometry assumed in these calculations is supported by constant-momentum-transfer-averaged (CMTA) LEED,[25] and angle-resolved x-ray photoemission measurements[13] which suggest that upon annealing Ag

embeds in the hollow sites at depths of -0.7 and -0.2 Å, respectively. Thus, although such calculations have not been done for the Cu/Si(111) interface, there is good reason to believe that the proposed geometry is energetically feasible.

Previous Si(111)($\sqrt{3}\times\sqrt{3}$)R30°-Ag surface structural studies indicate that interaction with Ag atoms significantly perturbs the positions of surface Si atoms both laterally and vertically.[13,25] The CMTA LEED intensity measurements suggest that the thickness of the first Si double layer is expanded by 0.75 Å and the distance between the second and third Si layer is contracted by 1.05 Å.[25] The photoelectron diffraction measurements indicate that a lateral expansion of the double-layer Si atoms occurs in directions away from the hollow sites containing Ag atoms.[13] Thus, it would appear that there is ample precedent for thinking that noble metals can significantly modify the Si(111) surface as bonding occurs.

VI. CONCLUSIONS

Through the use of high-energy Auger electron diffraction and associated kinematical scattering calculations, we have made a structural assignment for the surface of the annealed 1-ML Cu/Si(111) interface. Our results suggest that the Si surface reconstructs from the ideal Si(111) structure to a planar geometry with sixfold symmetry and that Cu atoms reside in the hollow sites at a depth of -0.1 ± 0.1 Å. The level of sensitivity of the method to structural details is high, thus providing a unique solution. Inasmuch as Auger electron scattering occurs primarily at nearest and next-nearest neighbor atoms, this technique is a short-range probe.

[1]S. D. Kevan, D. H. Rosenblatt, D. R. Denley, B.-C. Lu, and D. A. Shirley, Phys. Rev. B 20, 4133 (1979).
[2]S. Kono, S. M. Goldberg, N. F. T. Hall, and C. S. Fadley, Phys. Rev. B 22, 6085 (1980).
[3]P. J. Orders, S. Kono, C. S. Fadley, R. Trehan, and J. T. Lloyd, Surf. Sci. 119, 371 (1982).
[4]D. H. Rosenblatt, S. D. Kevan, J. G. Tobin, R. F. Davis, M. G. Mason, D. R. Denley, D. A. Shirley, Y. Huang, and S. Y. Tong, Phys. Rev. B 26, 1812 (1982).
[5]D. H. Rosenblatt, S. D. Kevan, J. G. Tobin, R. F. Davis, M. G. Mason, D. A. Shirley, J. C. Tang, and S. Y. Tong, Phys. Rev. B. 26, 3181 (1982).
[6]J. J. Barton, C. C. Bahr, Z. Hussain, S. W. Robey, J. G. Tobin, L. E. Klebanoff, and D. A. Shirley, Phys. Rev. Lett. 51, 272 (1983).
[7]E. L. Bullock, C. S. Fadley, and P. J. Orders, Phys. Rev. B 28, 4867 (1983).
[8]M. Owani, M. Kudo, Y. Nihei, and H. Kamada, J. Electron Spectrosc. 21, 131 (1981).
[9]P. J. Orders, R. E. Connelly, N. F. T. Hall, and C. S. Fadley,

Phys. Rev. B 24, 6163 (1981).
[10]S. A. Chambers and L. W. Swanson, Surf. Sci. 131, 385 (1983).
[11]W. F. Egelhoff, Jr., Phys. Rev. B 30, 1052 (1984).
[12]E. L. Bullock and C. S. Fadley, Phys. Rev. B 31, 1212 (1985).
[13]S. Kono, H. Sakurai, K. Higashiyama, and T. Sagawa, Surf. Sci. 130, L299 (1983).
[14]F. Ringeisen, J. Derrien, E. Daugy, J. M. Layet, P. Mathiez, and F. Salvan, J. Vac. Sci. Technol. B1, 546 (1983).
[15]C. S. Fadley, in Progress in Surface Science, edited by S. G. Davison (Pergamon, New York, in press).
[16]L. McDonnell, D. P. Woodruff, and B. W. Holland, Surf. Sci. 51, 249 (1975).
[17]M. Fink and J. Ingram, At. Data 4, 129 (1972).
[18]H. Gregory and M. Fink, At. Data Nucl. Data Tables 14, 39 (1974).
[19]N. W. Ashcroft and N. D. Mermin, Solid State Physics (Holt, Rinehart, and Winston, New York, 1976), p. 461.
[21]S. A. Chambers and J. H. Weaver (unpublished).
[22]F. Wehking, H. Beckermann, and R. Niedermayer, Surf. Sci.

71, 364 (1978).

[23]T. Yokotsuka, S. Kono, S. Suzuki, and T. Sagawa, Surf. Sci. 127, 35 (1983).

[24]T. Hoshino, Surf. Sci. 121, 1 (1982).

[25]Y. Terado, T. Yoshizuka, K. Oura, and T. Hanawa, Surf. Sci. 114, 65 (1982).